

Signature of magnetic phase separation in the ground state of $\text{Pr}_{1-x}\text{Ca}_x\text{MnO}_3$ Hao Sha,¹ F. Ye,² Pengcheng Dai,^{2,3} J. A. Fernandez-Baca,^{2,3} Dalgis Mesa,¹ J. W. Lynn,⁴ Y. Tomioka,⁵ Y. Tokura,^{5,6} and Jiandi Zhang^{1,*}¹Department of Physics, Florida International University, Miami, Florida 33199, USA²Neutron Scattering Science Division, Oak Ridge National Laboratory, Oak Ridge, Tennessee 37831-6393, USA³Department of Physics and Astronomy, The University of Tennessee, Knoxville, Tennessee 37996-1200, USA⁴NIST Center for Neutron Research, Gaithersburg, Maryland, 20899-6102, USA⁵Correlated Electron Research Center (CERC), National Institute of Advanced Industrial Science and Technology (AIST), Tsukuba 305-0046, Japan⁶Department of Applied Physics, University of Tokyo, Tokyo 113-8656, Japan

(Received 23 July 2008; published 27 August 2008)

Neutron scattering has been used to investigate the evolution of long- and short-range charge-ordered (CO), ferromagnetic, and antiferromagnetic (AF) correlations in single crystals of $\text{Pr}_{1-x}\text{Ca}_x\text{MnO}_3$. The existence and population of spin clusters as reflected by short-range correlations are found to drastically depend on the doping and temperature. Concentrated spin clusters coexist with long-range canted AF order in a wide temperature range in the $x=0.3$ while clusters do not appear in the $x=0.4$ crystal. In contrast, both CO and AF order parameters in the $x=0.35$ crystal show a precipitous decrease below ~ 35 K where spin clusters form. These results provide direct evidence of magnetic phase separation and demonstrate a critical doping x_c (close to $x=0.35$) that divides the inhomogeneous from homogeneous CO ground state.

DOI: 10.1103/PhysRevB.78.052410

PACS number(s): 75.47.Lx, 61.05.F-, 72.15.Gd

The $R_{1-x}A_x\text{MnO}_3$ (where R and A are rare- and alkaline-earth ions) manganites, known for the existence of “colossal” magnetoresistance, provide an archetype laboratory for the study of phase inhomogeneities.¹ In general, doping (x) not only causes a quenched disorder due to the size mismatch of A-site cations but also induces a distinctive chemical valence in Mn ions (Mn^{3+} vs Mn^{4+} in the original portrayal^{2,3}). These two kinds of Mn ions can assemble themselves into a CE-type checkerboardlike charge-ordered (CO) state at low temperature (LT) as shown in Fig. 1(b), promoting an antiferromagnetic (AF) insulating phase that competes with the ferromagnetic (FM) metallic state.⁴⁻⁶ In a conventional CO state, referred to as a site-centered CO structure, distinct Mn^{3+} and Mn^{4+} ions in half-doped manganites ($x=0.5$) form a 1:1 ratio. However, another possible CO pattern may also occur, namely, the bond-centered structure in which the charge is localized not on Mn sites but on Mn-O-Mn bonds with no distinctive $\text{Mn}^{3+}/\text{Mn}^{4+}$ sites,⁷⁻¹⁰ thus raising an unsettled issue about the nature of the ground state around $x=0.5$.¹¹

Furthermore, even in some non-half-doped ($x \neq 0.5$) manganites, an ostensible pseudo-type CO state has been reported.^{6,12-14} Within the CE-type CO frame, excess electronic charge (or Mn^{3+} ions) with respect to the ideal half-doped ($x=0.5$) case exists in these non-half-doped compounds. Consequently, important issues naturally emerge: how is the excessive electronic charge distributed in the CO state and what are the arrangements of spins and orbitals? There are at least three possible scenarios based on the charge distribution. First, the excessive electronic charge is distributed locally in the CE-type motif with distinct Mn^{3+} and Mn^{4+} sites. Apparently an electronic/magnetic phase separation is unavoidable due to unequal amounts of Mn^{3+} and Mn^{4+} ions while keeping the rigid CE-type Mn^{3+} and Mn^{4+} order. Another possibility is that the excessive charge is distributed uniformly in the CE-type motif with a certain

charge disproportionation.^{15,16} Both scenarios can be categorized as the site-centered structure because of having distinctive Mn sites, one inhomogeneous while the other homogeneous. The third scenario is a completely homogeneous bond-centered structure in which all Mn sites are

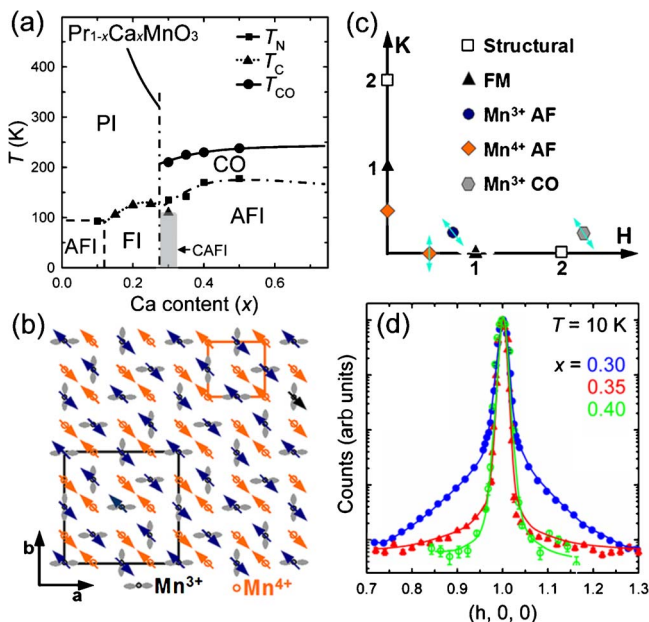


FIG. 1. (Color online) (a) Generic phase diagram of $\text{Pr}_{1-x}\text{Ca}_x\text{MnO}_3$ (Ref. 6). (b) Schematic ab -plane view of the CE-type structure with both orbital ($d_{3x^2-r^2}/d_{3y^2-r^2}$) and spin orderings. The bigger square denotes the Mn^{3+} orbital/magnetic unit cell while the smaller square shows the Mn^{4+} magnetic unit cell (c) The probed superlattice peak positions and the scan directions (marked by arrows) in reciprocal space. (d) Normalized q -scan profiles of the scattering near $(1, 0, 0)$ at $T=10$ K for PCMO30, PCMO35, and PCMO40. The solid lines are guides to the eye.

TABLE I. The integrated intensity ratios of the diffuse and total (diffuse plus Bragg) magnetic scattering [$\rho_{\text{FM,AF}} \equiv I_{\text{diffuse}}(\text{FM, AF})/I_{\text{total}}(\text{FM, AF})$] vs x measured at 10 K; ρ_{FM} , the ratio obtained from the scan across (1, 0, 0) by subtracting the lattice contribution to the Bragg peak; ρ_{AF} , the ratio obtained from the scan across (0.5, 0, 0).

$\text{Pr}_{1-x}\text{Ca}_x\text{MnO}_3$	$x=0.30$	$x=0.35$	$x=0.40$
$T_{\text{CO}}; T_{\text{N}}; T_{\text{C}}$ (K)	210; 125; 10	230; 160; N/A	245; 170; N/A
$\rho_{\text{FM}}; (\times 100\%)$	15.1 ± 2.0	N/A	N/A
$\rho_{\text{AF}}; (\times 100\%)$	28.7 ± 0.8	0.160 ± 0.003	N/A

equivalent.^{7,17} Presently it is unclear which scenario is more appropriate for the observed CO state. Alternatively, could it be possible that the CO structure depends on doping concentration?

In this work, we report the signature of magnetic phase separation in the CO state from neutron-scattering studies of a prototype manganite system: $\text{Pr}_{1-x}\text{Ca}_x\text{MnO}_3$ (PCMO). PCMO has negligible quenched disorder since Pr^{3+} and Ca^{2+} have almost equal ionic radii. As shown in Fig. 1(a), the nonmetallic CO ground state of PCMO exists over a broad doping range ($0.3 \leq x \leq 0.7$).⁶ We have discovered a critical doping concentration x_c that separates the inhomogeneous and homogeneous CO ground states, thus providing direct evidence on how doping affects the CO structure.

Three single crystals with $x=0.3$ (PCMO30), 0.35 (PCMO35), and 0.4 (PCMO40) were grown by the floating-zone method.⁶ The measurements were carried out using the HB-1 and HB-3 triple-axis spectrometers at the High Flux Isotope Reactor at the Oak Ridge National Laboratory (ORNL) and BT-7 and BT-9 at the NIST Center for Neutron Research. For simplicity, we label all wave vectors in terms of the pseudocubic unit cell with lattice parameters of $a = 3.87 \text{ \AA}$, although all of our samples have orthorhombic structures slightly distorted from the cubic lattice. The wave vector $\mathbf{Q}=(Q_x, Q_y, Q_z)$ is in units of \AA^{-1} and $(H, K, L) = (Q_x a/2\pi, Q_y a/2\pi, Q_z a/2\pi)$ is in reciprocal-lattice units (rlus). The samples were aligned to allow the wave vector in the form of $(H, K, 0)$ accessible in the horizontal scattering plane.

All of the measurements were based upon the CE-type structure with CO and AF ordering shown in Fig. 1(b). Including the orbital part, the periodicity of AF order for Mn^{3+} spins is twice of that for Mn^{4+} spins. As shown in Fig. 1(c),¹⁸ we used $\mathbf{Q}=(2.25, 0.25, 0)$, (1, 0, 0), (0.75, 0.25, 0), and (0.5, 0, 0) to probe the order of the CO, FM, and AF at Mn^{3+} and Mn^{4+} sites, respectively. The corresponding short-range correlations or, alternatively, clusters, were also determined by measuring the diffuse scattering around these characteristic positions.¹⁹ As listed in Table I, the measured transition temperatures for CO, AF, and FM phases are in agreement with those reported in the literature. A canted long-range FM order coexists with an AF structure in PCMO30 below $T_{\text{C}} = 110\text{K}$ [see inset (a) of Fig. 2], known as a canted AF insulating (CAFI) phase.²⁰ However, no long-range FM order was detected in the ground state for either PCMO35 or PCMO40.

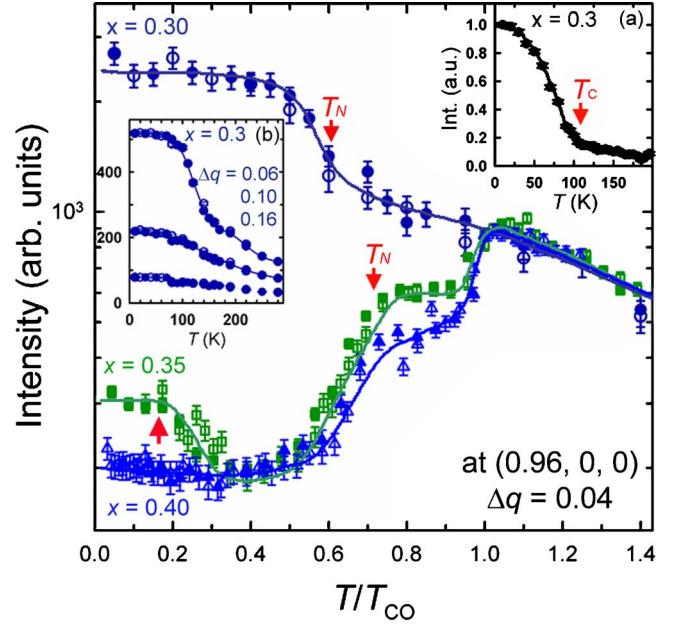


FIG. 2. (Color online) T dependence of the FM diffuse component measured at (0.96, 0, 0) ($\Delta q=0.04$ rlu) for different x 's of $\text{Pr}_{1-x}\text{Ca}_x\text{MnO}_3$ on cooling (solid symbols) and warming (open symbols). The solid curves are guides to the eye. Arrows mark the Curie and Néel temperatures, as well as the onset of spin phase separation for PCMO35. The insets present the T dependence of (a) the FM order parameter (Bragg-peak intensity) and (b) the FM diffuse component at selected q positions from (1, 0, 0) for PCMO30.

We observed a strong doping dependence of both AF and FM diffuse scattering in the ground state. Figure 1(d) displays the normalized q scans at (1, 0, 0) including both magnetic and structural scatterings from the three doping levels. Similar to those reported before,^{20,21} a strong diffuse component appears near the Bragg peak for PCMO30, which indicates that FM spin clusters coexist with the long-range FM order in the ground state. In contrast, PCMO35 has a rather weak FM diffuse shoulder. PCMO40 shows only a nice Gaussian profile due to long-range lattice scattering with no sign of short-range spin correlations. The AF scattering profiles at (0.5, 0, 0) and (0.75, 0.25, 0) reveal a similar x dependence of diffuse components. As summarized in Table I, PCMO30 has a CAFI ground state with a significant amount of FM/AF clusters ($\rho_{\text{FM}} \approx 15.1 \pm 2.0\%$ and $\rho_{\text{AF}} \approx 28.7 \pm 0.8\%$). PCMO35 has an almost homogeneous AF ground state with a very small weight of spin clusters, and PCMO40 has a completely uniform AF ground state. Therefore, a critical doping x_c must exist and be very close to the value of $x=0.35$, which serves as the boundary between the homogeneous and inhomogeneous ground state of $\text{Pr}_{1-x}\text{Ca}_x\text{MnO}_3$.

To further reveal such a critical doping behavior for the inhomogeneity in the magnetic structure, we have examined the T dependence of the FM diffuse scattering intensity at $\mathbf{Q}=(0.96, 0, 0)$, which is outside the influence of the Bragg peak for long-range ordering. Figure 2 presents the measured intensity as a function of T/T_{CO} for all three doping levels. Similar behavior is obtained for different positions [see inset (b) of Fig. 2]. The FM diffuse component clearly displays a

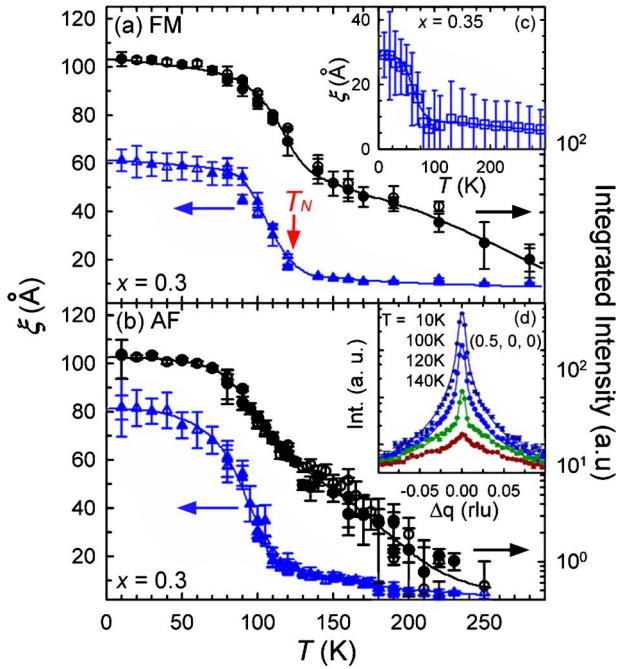


FIG. 3. (Color online) T dependence of the intensity and extracted short-range correlation length of (a) FM at $(1, 0, 0)$ and (b) Mn^{4+} AF at $(0.5, 0, 0)$ in PCMO30. The solid lines are guides to the eye. The solid symbols are for cooling while open symbols for warming. The insets show the T dependence of (c) FM short-range correlation length in PCMO35 with large error bars due to the weak diffuse scattering profiles and (d) q scans of Mn^{4+} AF at $(0.5, 0, 0)$ in PCMO30.

different T dependence above and below T_{CO} . Comparable results have also been reported by Kajimoto *et al.*²¹ When $T > T_{\text{CO}}$, all three doping levels of crystals exhibit a similar T dependence of the diffuse component, reflecting the FM spin fluctuations in the paramagnetic phase, which are presumably induced by double-exchange (DE) interaction.¹

On the other hand, a completely different T dependence of the diffuse components for different doping levels appears below T_{CO} . For PCMO40, the FM spin fluctuations deteriorate below T_{CO} and vanish below T_N . In principle, such a T dependence in PCMO40 can be understood as follows. When $T < T_{\text{CO}}$, the DE-mediated FM spin fluctuations will be suppressed by the charge localization. When $T < T_N$, the FM fluctuations diminish further because of the onset of AF order. For PCMO35, the FM spin fluctuations exhibit the same T dependence as those in PCMO40, thus indicating that they originate from the same mechanism. However, spin clusters appear below ~ 65 K with both FM (see Fig. 2) and AF characters, as reflected by the corresponding diffuse components. This is distinctive from the FM spin fluctuations at high temperature. In sharp contrast with those in both PCMO35 and PCMO40, the population of spin clusters in PCMO30, reflected by the intensity of the FM diffuse component, increases rather than decreases below T_{CO} . Surprisingly, it increases much more drastically below T_N , regardless of the establishment of AF order, thus suggesting the spin clusters in the ground state may have a different nature from the DE-mediated FM fluctuations at high temperature.

The spin clusters appearing in PCMO30 in the LT regime also display both FM and AF characters, similar to those existing in the ground state of PCMO35. The integrated diffuse scattering intensity and the extracted short-range correlation length ξ near the FM and AF peaks exhibit very similar T dependence (see Fig. 3). The measured average cluster diameter (i.e., correlation length) is $\xi_{\text{FM}} \approx 60$ Å from FM and $\xi_{\text{AF}} \approx 80$ Å from AF scattering. Using a simple estimated population relation in the ab plane of the crystal, $\rho_{\text{FM,AF}} \propto n_{\text{FM,AF}} \xi_{\text{FM,AF}}^2$, where $n_{\text{FM,AF}}$ is the in-plane cluster density, we find that $n_{\text{FM}} \cong n_{\text{AF}}$ with measured $\rho_{\text{FM,AF}}$ (Table I), regardless of the difference in correlation length. Therefore, we speculate that the measured AF and FM diffuse scatterings may be indeed caused from the same assembly of spin clusters.

Due to the fairly weak diffuse scattering and uncertain correlation length [see inset (c) of Fig. 3] we were not able to do a similar estimation for PCMO35. Nevertheless, the ground state in both PCMO30 and PCMO35 is a phase-separated state containing spin clusters embedded in either an AF or a canted AF ordered matrix. The main difference between these two doping levels is that the magnetic phase separation exists in the entire measured temperature range in PCMO30 but appears with much smaller population only at LT in PCMO35. One can anticipate that such a phase-separated ground state will disappear in a crystal of $\text{Pr}_{1-x}\text{Ca}_x\text{MnO}_3$ with a doping level slightly larger than $x = 0.35$. Such an evolution of phase separation with doping may provide insight into the doping dependence of the observed CMR effect.⁶ This evolution may also explain why a smaller critical magnetic field is sufficient to melt the CO

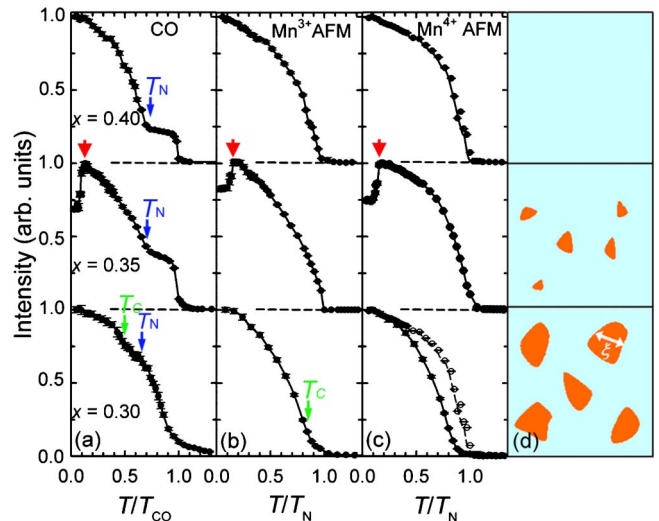


FIG. 4. (Color online) T dependence of order parameters for (a) CO structure measured at $(2.25, 0.25, 0)$, (b) Mn^{3+} AFM ordering at $(0.75, 0.25, 0)$, and (c) Mn^{4+} AFM ordering at $(0.5, 0, 0)$ for the three doping x 's of $\text{Pr}_{1-x}\text{Ca}_x\text{MnO}_3$. The Mn^{4+} AFM order parameters for both $x=0.3$ and 0.4 (open dots) are plotted together in the bottom of panel (c) for comparison. Arrows mark the onset of phase separation for PCMO35. Column (d) illustrates the evolution from an inhomogeneous to a homogeneous CO ground state for corresponding doping levels. A T -induced change from homogeneous to inhomogeneous phase occurs in PCMO35.

state for PCMO30 than that for PCMO35 and PCMO40.

If indeed PCMO35 is a system which undergoes a phase evolution from homogeneous to inhomogeneous spin-ordered state on cooling, then the appearance of spin clusters at LT should affect the long-range order parameters. To elucidate this issue we have investigated systematically the order parameters of the CO and AF at both Mn^{3+} and Mn^{4+} sites, respectively. As clearly shown in Fig. 4, an anomaly characterized by a sudden drop in the intensity of the measured order parameters in PCMO35 emerges at ~ 35 K, coinciding with the establishment of spin clusters and thus providing a clear signature of magnetic phase separation. In addition, we note that the line shape of these order parameters in PCMO30 near both T_{CO} and T_N is slightly different from that in PCMO35 and PCMO40. The transitions in PCMO35 and PCMO40 show more pronounced critical behavior than those in PCMO30. The nature behind this should be associated with the existence of phase separation near T_N and T_{CO} in PCMO30, which does not occur in the other two doping levels.

In summary, we have observed strong x and T dependences of magnetic phase separation in $\text{Pr}_{1-x}\text{Ca}_x\text{MnO}_3$ crystals. Spin clusters with both AF and FM correlations coexist with a CAFI structure in PCMO30, suggesting an inhomogeneous CO state below T_{CO} . In contrast, the observed uniform AF ordered structure suggests a homogeneous AF CO state in PCMO40. We have identified a critical doping x_c , which is very close to $x=0.35$, to divide homogeneous and inhomogeneous CO ground states. Whether the homogeneous CO state in PCMO40 is a site- or bond-centered type is still unclear. One possible experimental method to distinguish these two types of CO structures is resonant x-ray scattering.²² Yet, it is clear that in a manganite away from half doping, a CE-type $\text{Mn}^{3+}/\text{Mn}^{4+}$ CO state cannot survive without phase separation.

This work was supported by the U.S. DOE FG02-04ER46125 and NSF DMR-0346826. P.D. was supported by U.S. NSF DMR-0756568. ORNL is managed by UT-Battelle, LLC, for the U.S. DOE DE-AC05-00OR22725.

*zhangj@fiu.edu

- ¹E. Dagotto, *Nanoscale Phase Separation and Colossal Magnetoresistance* (Springer, Berlin, 2002); *Science* **309**, 257 (2005).
- ²E. O. Wollan and W. C. Koehler, *Phys. Rev.* **100**, 545 (1955).
- ³J. B. Goodenough, *Phys. Rev.* **100**, 564 (1955).
- ⁴Z. Jirák, S. Krupicka, V. Nekvasil, E. Pollert, G. Villeneuve, and F. Zounova, *J. Magn. Magn. Mater.* **15-18**, 519 (1980).
- ⁵Y. Tokura, H. Kuwahara, Y. Moritomo, Y. Tomioka, and A. Asamitsu, *Phys. Rev. Lett.* **76**, 3184 (1996); Y. Tokura and N. Nagaosa, *Science* **288**, 462 (2000).
- ⁶Y. Tomioka, A. Asamitsu, H. Kuwahara, Y. Moritomo, and Y. Tokura, *Phys. Rev. B* **53**, R1689 (1996).
- ⁷A. Daoud-Aladine, J. Rodriguez-Carvajal, L. Pinsard-Gaudart, M. T. Fernandez-Diaz, and A. Revcolevschi, *Phys. Rev. Lett.* **89**, 097205 (2002).
- ⁸V. Ferrari, M. Towler, and P. B. Littlewood, *Phys. Rev. Lett.* **91**, 227202 (2003).
- ⁹G. Zheng and C. H. Patterson, *Phys. Rev. B* **67**, 220404(R) (2003).
- ¹⁰C. Zener, *Phys. Rev.* **82**, 403 (1951); J.-S. Zhou and J. B. Goodenough, *Phys. Rev. B* **62**, 3834 (2000).
- ¹¹D. V. Efremov, J. van den Brink, and D. I. Khomskii, *Nat. Mater.* **3**, 853 (2004).
- ¹²E. Pollert, S. Krupicka, and E. Kuzmicova, *J. Phys. Chem. Solids* **43**, 1137 (1982).
- ¹³T. Asaka, S. Yamada, S. Tsutsumi, C. Tsuruta, K. Kimoto, T. Arima, and Y. Matsui, *Phys. Rev. Lett.* **88**, 097201 (2002); Y. Tokura, *Rep. Prog. Phys.* **69**, 797 (2006).
- ¹⁴D. E. Cox, P. G. Radaelli, M. Marezio, and S. W. Cheong, *Phys. Rev. B* **57**, 3305 (1998); M. von Zimmermann, C. S. Nelson, J. P. Hill, D. Gibbs, M. Blume, D. Casa, B. Keimer, Y. Murakami, C. C. Kao, C. Venkataraman, T. Gog, Y. Tomioka, and Y. Tokura, *ibid.* **64**, 195133 (2001).
- ¹⁵J. van den Brink, G. Khaliullin, and D. Khomskii, *Phys. Rev. Lett.* **83**, 5118 (1999); Z. Popović and S. Satpathy, *ibid.* **88**, 197201 (2002).
- ¹⁶S. Grenier, J. P. Hill, D. Gibbs, K. J. Thomas, M. von Zimmermann, C. S. Nelson, V. Kiryukhin, Y. Tokura, Y. Tomioka, D. Casa, T. Gog, and C. Venkataraman, *Phys. Rev. B* **69**, 134419 (2004).
- ¹⁷Ch. Jooss, L. Wu, T. Beetz, R. F. Klie, M. Beleggia, M. A. Schofield, S. Schramm, J. Hoffmann, and Y. Zhu, *Proc. Natl. Acad. Sci. U.S.A.* **104**, 13597 (2007).
- ¹⁸F. Ye, J. A. Fernandez-Baca, P. Dai, J. W. Lynn, H. Kawano-Furukawa, H. Yoshizawa, Y. Tomioka, and Y. Tokura, *Phys. Rev. B* **72**, 212404 (2005).
- ¹⁹The diffuse components of scattering were fitted to Lorentzian line shapes convoluted with the instrumental resolution. The linewidth Γ corresponds to the inverse correlation length ($\Gamma = 1/\xi$), where ξ is also the spin cluster size. The intensity of the Lorentzians is proportional to the population of spin clusters.
- ²⁰H. Yoshizawa, H. Kawano, Y. Tomioka, and Y. Tokura, *Phys. Rev. B* **52**, R13145 (1995); P. G. Radaelli, R. M. Ibberson, D. N. Argyriou, H. Casalta, K. H. Andersen, S. W. Cheong, and J. F. Mitchell, *ibid.* **63**, 172419 (2001); J. A. Fernandez-Baca, P. Dai, H. Kawano-Furukawa, H. Yoshizawa, E. W. Plummer, S. Katano, Y. Tomioka, and Y. Tokura, *ibid.* **66**, 054434 (2002).
- ²¹R. Kajimoto, T. Kakeshita, Y. Oohara, H. Yoshizawa, Y. Tomioka, and Y. Tokura, *Phys. Rev. B* **58**, R11837 (1998).
- ²²P. Abbamonte, *Phys. Rev. B* **74**, 195113 (2006).